Cross sections measurement of $e^+e^- \to \Xi(1530)^0\bar{\Xi}^0 + \mathrm{c.c.}$ and search for $\psi(3770) \to \Xi(1530)^0\bar{\Xi}^0 + \mathrm{c.c.}$

M. Ablikim,[1] M. N. Achasov,[4,b] P. Adlarson,[79] X. C. Ai,[84] R. Aliberti,[37] A. Amoroso,[78a,78c] Q. An,[75,61,a] Y. Bai,[60] O. Bakina,[38] Y. Ban,[48,c] H.-R. Bao,[67] V. Batozskaya,[1,46] K. Begzsuren,[34] N. Berger,[37] M. Berlowski,[46] M. B. Bertani,[30a] D. Bettoni,[31a] F. Bianchi,[78a,78c] E. Bianco,[78a,78c] A. Bortone,[78a,78c] I. Boyko,[38] R. A. Briere,[5] A. Brueggemann,[72] H. Cai,[80] M. H. Cai,[40,d,e] X. Cai,[1,61] A. Calcaterra,[30a] G. F. Cao,[1,67] N. Cao,[1,67] S. A. Cetin,[65a] X. Y. Chai,[48,c] J. F. Chang,[1,61] T. T. Chang,[45] G. R. Che,[45] Y. Z. Che,[1,61,67] C. H. Chen,[9] Chao Chen,[58] G. Chen,[1] H. S. Chen,[1,67] H. Y. Chen,[21] M. L. Chen,[1,61,67] S. J. Chen,[44] S. M. Chen,[64] T. Chen,[1,67] X. R. Chen,[33,67] X. T. Chen,[1,67] X. Y. Chen,[12,f] Y. B. Chen,[1,61] Y. Q. Chen,[16] Z. K. Chen,[62] J. C. Cheng,[47] L. N. Cheng,[45] S. K. Choi,[10] X. Chu,[12,f] G. Cibinetto,[31a] F. Cossio,[78c] J. Cottee-Meldrum,[66] H. L. Dai,[1,61] J. P. Dai,[82] X. C. Dai,[64] A. Dbeyssi,[19] R. E. de Boer,[3] D. Dedovich,[38] C. Q. Deng,[76] Z. Y. Deng,[1] A. Denig,[37] I. Denisenko,[38] M. Destefanis,[78a,78c] F. De Mori,[78a,78c] X. X. Ding,[48,c] Y. Ding,[42] Y. X. Ding,[32] J. Dong,[1,61] L. Y. Dong,[1,67] M. Y. Dong,[1,61,67] X. Dong,[80] M. C. Du,[1] S. X. Du,[84] S. X. Du,[12,f] X. L. Du,[84] Y. Y. Duan,[58] Z. H. Duan,[44] P. Egorov,[38,g] G. F. Fan,[44] J. J. Fan,[20] Y. H. Fan,[47] J. Fang,[1,61] J. Fang,[62] S. S. Fang,[1,67] W. X. Fang,[1] Y. Q. Fang,[1,61] L. Fava,[78b,78c] F. Feldbauer,[3] G. Felici,[30a] C. Q. Feng,[75,61] J. H. Feng,[16] L. Feng,[40,d,e] Q. X. Feng,[40,d,e] Y. T. Feng,[75,61] M. Fritsch,[3] C. D. Fu,[1] J. L. Fu,[67] Y. W. Fu,[1,67] H. Gao,[67] Y. Gao,[75,61] Y. N. Gao,[48,c] Y. N. Gao,[20] Y. Y. Gao,[32] Z. Gao,[45] S. Garbolino,[78c] I. Garzia,[31a,31b] L. Ge,[60] P. T. Ge,[20] Z. W. Ge,[44] C. Geng,[62] E. M. Gersabeck,[71] A. Gilman,[73] K. Goetzen,[13] J. D. Gong,[36] L. Gong,[42] W. X. Gong,[1,61] W. Gradl,[37] S. Gramigna,[31a,31b] M. Greco,[78a,78c] M. D. Gu,[53] M. H. Gu,[1,61] C. Y. Guan,[1,67] A. Q. Guo,[33] J. N. Guo,[12,f] L. B. Guo,[43] M. J. Guo,[52] R. P. Guo,[51] X. Guo,[52] Y. P. Guo,[12,f] A. Guskov,[38,g] J. Gutierrez,[29] T. T. Han,[1] F. Hanisch,[3] K. D. Hao,[75,61] X. Q. Hao,[20] F. A. Harris,[69] C. Z. He,[48,c] K. L. He,[1,67] F. H. Heinsius,[3] C. H. Heinz,[37] Y. K. Heng,[1,61,67] C. Herold,[63] P. C. Hong,[36] G. Y. Hou,[1,67] X. T. Hou,[1,67] Y. R. Hou,[67] Z. L. Hou,[1] H. M. Hu,[1,67] J. F. Hu,[59,h] Q. P. Hu,[75,61] S. L. Hu,[12,f] T. Hu,[1,61,67] Y. Hu,[1] Z. M. Hu,[62] G. S. Huang,[75,61] K. X. Huang,[62] L. Q. Huang,[33,67] P. Huang,[44] X. T. Huang,[52] Y. P. Huang,[1] Y. S. Huang,[62] T. Hussain,[77] N. Hüsken,[37] N. in der Wiesche,[72] J. Jackson,[29] Q. Ji,[1] Q. P. Ji,[20] W. Ji,[1,67] X. B. Ji,[1,67] X. L. Ji,[1,61] X. Q. Jia,[52] Z. K. Jia,[75,61] D. Jiang,[1,67] H. B. Jiang,[80] P. C. Jiang,[48,c] S. J. Jiang,[9] X. S. Jiang,[1,61,67] Y. Jiang,[67] J. B. Jiao,[52] J. K. Jiao,[36] Z. Jiao,[25] S. Jin,[44] Y. Jin,[70] M. Q. Jing,[1,67] X. M. Jing,[67] T. Johansson,[79] S. Kabana,[35] N. Kalantar-Nayestanaki,[68] X. L. Kang,[9] X. S. Kang,[42] M. Kavatsyuk,[68] B. C. Ke,[84] V. Khachatryan,[29] A. Khoukaz,[72] O. B. Kolcu,[65a] B. Kopf,[3] M. Kuessner,[3] X. Kui,[1,67] N. Kumar,[28] A. Kupsc,[46,79] W. Kühn,[39] Q. Lan,[76] W. N. Lan,[20] T. T. Lei,[75,61] M. Lellmann,[37] T. Lenz,[37] C. Li,[49] C. Li,[45] C. H. Li,[43] C. K. Li,[21] D. M. Li,[84] F. Li,[1,61] G. Li,[1] H. B. Li,[1,67] H. J. Li,[20] H. L. Li,[84] H. N. Li,[59,h] Hui Li,[45] J. R. Li,[64] J. S. Li,[62] J. W. Li,[52] K. Li,[1] K. L. Li,[40,d,e] L. J. Li,[1,67] Lei Li,[50] M. H. Li,[45] M. R. Li,[1,67] P. L. Li,[67] P. R. Li,[40,d,e] Q. M. Li,[1,67] Q. X. Li,[52] R. Li,[18,33] S. X. Li,[12] Shanshan Li,[27,i] T. Li,[52] T. Y. Li,[45] W. D. Li,[1,67] W. G. Li,[1,a] X. Li,[1,67] X. H. Li,[75,61] X. K. Li,[48,c] X. L. Li,[52] X. Y. Li,[1,8] X. Z. Li,[62] Y. Li,[20] Y. G. Li,[48,c] Y. P. Li,[36] Z. H. Li,[40] Z. J. Li,[62] Z. X. Li,[45] Z. Y. Li,[82] C. Liang,[44] H. Liang,[75,61] Y. F. Liang,[57] Y. T. Liang,[33,67] G. R. Liao,[14] L. B. Liao,[62] M. H. Liao,[62] Y. P. Liao,[1,67] J. Libby,[28] A. Limphirat,[63] D. X. Lin,[33,67] L. Q. Lin,[41] T. Lin,[1] B. J. Liu,[1] B. X. Liu,[80] C. X. Liu,[1] F. Liu,[1] F. H. Liu,[56] Feng Liu,[6] G. M. Liu,[59,h] H. Liu,[40,d,e] H. B. Liu,[15] H. H. Liu,[1] H. M. Liu,[1,67] Huihui Liu,[22] J. B. Liu,[75,61] J. J. Liu,[21] K. Liu,[40,d,e] K. Liu,[76] K. Y. Liu,[42] Ke Liu,[23] L. Liu,[40] L. C. Liu,[45] Lu Liu,[45] M. H. Liu,[36] P. L. Liu,[1] Q. Liu,[67] S. B. Liu,[75,61] W. M. Liu,[75,61] W. T. Liu,[41] X. Liu,[40,d,e] X. K. Liu,[40,d,e] X. L. Liu,[12,f] X. Y. Liu,[80] Y. Liu,[40,d,e] Y. Liu,[84] Y. B. Liu,[45] Z. A. Liu,[1,61,67] Z. D. Liu,[9] Z. Q. Liu,[52] Z. Y. Liu,[40] X. C. Lou,[1,61,67] H. J. Lu,[25] J. G. Lu,[1,61] X. L. Lu,[16] Y. Lu,[7] Y. H. Lu,[1,67] Y. P. Lu,[1,61] Z. H. Lu,[1,67] C. L. Luo,[43] J. R. Luo,[62] J. S. Luo,[1,67] M. X. Luo,[83] T. Luo,[12,f] X. L. Luo,[1,61] Z. Y. Lv,[23] X. R. Lyu,[67,j] Y. F. Lyu,[45] Y. H. Lyu,[84] F. C. Ma,[42] H. L. Ma,[1] Heng Ma,[27,i] J. L. Ma,[1,67] L. L. Ma,[52] L. R. Ma,[70] Q. M. Ma,[1] R. Q. Ma,[1,67] R. Y. Ma,[20] T. Ma,[75,61] X. T. Ma,[1,67] X. Y. Ma,[1,61] Y. M. Ma,[33] F. E. Maas,[19] I. MacKay,[73] M. Maggiora,[78a,78c] S. Malde,[73] Q. A. Malik,[77] H. X. Mao,[40,d,e] Y. J. Mao,[48,c] Z. P. Mao,[1] S. Marcello,[78a,78c] A. Marshall,[66] F. M. Melendi,[31a,31b] Y. H. Meng,[67] Z. X. Meng,[70] G. Mezzadri,[31a] H. Miao,[1,67] T. J. Min,[44] R. E. Mitchell,[29] X. H. Mo,[1,61,67] B. Moses,[29] N. Yu. Muchnoi,[4,b] J. Muskalla,[37] Y. Nefedov,[38] F. Nerling,[19,k] Z. Ning,[1,61] S. Nisar,[11,l] Q. L. Niu,[40,d,e] W. D. Niu,[12,f] Y. Niu,[52] C. Normand,[66] S. L. Olsen,[10,67] Q. Ouyang,[1,61,67] S. Pacetti,[30b,30c] X. Pan,[58] Y. Pan,[60] A. Pathak,[10] Y. P. Pei,[75,61] M. Pelizaeus,[3] H. P. Peng,[75,61] X. J. Peng,[40,d,e] Y. Y. Peng,[40,d,e] K. Peters,[13,k] K. Petridis,[66] J. L. Ping,[43] R. G. Ping,[1,67] S. Plura,[37] V. Prasad,[36] F. Z. Qi,[1] H. R. Qi,[64] M. Qi,[44] S. Qian,[1,61] W. B. Qian,[67] C. F. Qiao,[67]

J. H. Qiao,[20] J. J. Qin,[76] J. L. Qin,[58] L. Q. Qin,[14] L. Y. Qin,[75,61] P. B. Qin,[76] X. P. Qin,[41] X. S. Qin,[52] Z. H. Qin,[1,61] J. F. Qiu,[1] Z. H. Qu,[76] J. Rademacker,[66] C. F. Redmer,[37] A. Rivetti,[78c] M. Rolo,[78c] G. Rong,[1,67] S. S. Rong,[1,67] F. Rosini,[30b,30c] Ch. Rosner,[19] M. Q. Ruan,[1,61] N. Salone,[46,m] A. Sarantsev,[38,n] Y. Schelhaas,[37] K. Schoenning,[79] M. Scodeggio,[31a] W. Shan,[26] X. Y. Shan,[75,61] Z. J. Shang,[40,d,e] J. F. Shangguan,[17] L. G. Shao,[1,67] M. Shao,[75,61] C. P. Shen,[12,f] H. F. Shen,[1,8] W. H. Shen,[67] X. Y. Shen,[1,67] B. A. Shi,[67] H. Shi,[75,61] J. L. Shi,[12,f] J. Y. Shi,[1] S. Y. Shi,[76] X. Shi,[1,61] H. L. Song,[75,61] J. J. Song,[20] M. H. Song,[40] T. Z. Song,[62] W. M. Song,[36] Y. X. Song,[48,c,o] Zirong Song,[27,i] S. Sosio,[78a,78c] S. Spataro,[78a,78c] S. Stansilaus,[73] F. Stieler,[37] S. S. Su,[42] G. B. Sun,[80] G. X. Sun,[1] H. Sun,[67] H. K. Sun,[1] J. F. Sun,[20] K. Sun,[64] L. Sun,[80] R. Sun,[75] S. S. Sun,[1,67] T. Sun,[54,p] W. Y. Sun,[53] Y. C. Sun,[80] Y. H. Sun,[32] Y. J. Sun,[75,61] Y. Z. Sun,[1] Z. Q. Sun,[1,67] Z. T. Sun,[52] C. J. Tang,[57] G. Y. Tang,[1] J. Tang,[62] J. J. Tang,[75,61] L. F. Tang,[41] Y. A. Tang,[80] L. Y. Tao,[76] M. Tat,[73] J. X. Teng,[75,61] J. Y. Tian,[75,61] W. H. Tian,[62] Y. Tian,[33] Z. F. Tian,[80] I. Uman,[65b] B. Wang,[1] B. Wang,[62] Bo Wang,[75,61] C. Wang,[40,d,e] C. Wang,[20] Cong Wang,[23] D. Y. Wang,[48,c] H. J. Wang,[40,d,e] J. Wang,[9] J. J. Wang,[80] J. P. Wang,[52] K. Wang,[1,61] L. L. Wang,[1] L. W. Wang,[36] M. Wang,[52] M. Wang,[75,61] N. Y. Wang,[67] S. Wang,[12,f] S. Wang,[40,d,e] T. Wang,[12,f] T. J. Wang,[45] W. Wang,[62] W. P. Wang,[37] X. Wang,[48,c] X. F. Wang,[40,d,e] X. L. Wang,[12,f] X. N. Wang,[1,67] Xin Wang,[27,i] Y. Wang,[1] Y. D. Wang,[47] Y. F. Wang,[1,8,67] Y. H. Wang,[40,d,e] Y. J. Wang,[75,61] Y. L. Wang,[20] Y. N. Wang,[47] Y. N. Wang,[80] Yaqian Wang,[18] Yi Wang,[64] Yuan Wang,[18,33] Z. Wang,[1,61] Z. Wang,[45] Z. L. Wang,[2] Z. Q. Wang,[12,f] Z. Y. Wang,[1,67] Ziyi Wang,[67] D. Wei,[45] D. H. Wei,[14] H. R. Wei,[45] F. Weidner,[72] S. P. Wen,[1] U. Wiedner,[3] G. Wilkinson,[73] M. Wolke,[79] J. F. Wu,[1,8] L. H. Wu,[1] L. J. Wu,[1,67] L. J. Wu,[20] Lianjie Wu,[20] S. G. Wu,[1,67] S. M. Wu,[67] X. Wu,[12,f] Y. J. Wu,[33] Z. Wu,[1,61] L. Xia,[75,61] B. H. Xiang,[1,67] D. Xiao,[40,d,e] G. Y. Xiao,[44] H. Xiao,[76] Y. L. Xiao,[12,f] Z. J. Xiao,[43] C. Xie,[44] K. J. Xie,[1,67] Y. Xie,[52] Y. G. Xie,[1,61] Y. H. Xie,[6] Z. P. Xie,[75,61] T. Y. Xing,[1,67] C. J. Xu,[62] G. F. Xu,[1] H. Y. Xu,[2] M. Xu,[75,61] Q. J. Xu,[17] Q. N. Xu,[32] T. D. Xu,[76] X. P. Xu,[58] Y. Xu,[12,f] Y. C. Xu,[81] Z. S. Xu,[67] F. Yan,[24] L. Yan,[12,f] W. B. Yan,[75,61] W. C. Yan,[84] W. H. Yan,[6] W. P. Yan,[20] X. Q. Yan,[1,67] H. J. Yang,[54,p] H. L. Yang,[36] H. X. Yang,[1] J. H. Yang,[44] R. J. Yang,[20] Y. Yang,[12,f] Y. H. Yang,[44] Y. Q. Yang,[9] Y. Z. Yang,[20] Z. P. Yao,[52] M. Ye,[1,61] M. H. Ye,[8,a] Z. J. Ye,[59,h] Junhao Yin,[45] Z. Y. You,[62] B. X. Yu,[1,61,67] C. X. Yu,[45] G. Yu,[13] J. S. Yu,[27,i] L. W. Yu,[12,f] T. Yu,[76] X. D. Yu,[48,c] Y. C. Yu,[84] Y. C. Yu,[40] C. Z. Yuan,[1,67] H. Yuan,[1,67] J. Yuan,[36] J. Yuan,[47] L. Yuan,[2] M. K. Yuan,[12,f] S. H. Yuan,[76] Y. Yuan,[1,67] C. X. Yue,[41] Ying Yue,[20] A. A. Zafar,[77] F. R. Zeng,[52] S. H. Zeng,[66] X. Zeng,[12,f] Yujie Zeng,[62] Y. J. Zeng,[1,67] Y. C. Zhai,[52] Y. H. Zhan,[62] Shunan Zhang,[73] B. L. Zhang,[1,67] B. X. Zhang,[1,a] D. H. Zhang,[45] G. Y. Zhang,[20] G. Y. Zhang,[1,67] H. Zhang,[75,61] H. Zhang,[84] H. C. Zhang,[1,61,67] H. H. Zhang,[62] H. Q. Zhang,[1,61,67] H. R. Zhang,[75,61] H. Y. Zhang,[1,61] J. Zhang,[62] J. J. Zhang,[55] J. L. Zhang,[21] J. Q. Zhang,[43] J. S. Zhang,[12,f] J. W. Zhang,[1,61,67] J. X. Zhang,[40,d,e] J. Y. Zhang,[1] J. Z. Zhang,[1,67] Jianyu Zhang,[67] L. M. Zhang,[64] Lei Zhang,[44] N. Zhang,[84] P. Zhang,[1,8] Q. Zhang,[20] Q. Y. Zhang,[36] R. Y. Zhang,[40,d,e] S. H. Zhang,[1,67] Shulei Zhang,[27,i] X. M. Zhang,[1] X. Y. Zhang,[52] Y. Zhang,[1] Y. Zhang,[76] Y. T. Zhang,[84] Y. H. Zhang,[1,61] Y. P. Zhang,[75,61] Z. D. Zhang,[1] Z. H. Zhang,[1] Z. L. Zhang,[36] Z. L. Zhang,[58] Z. X. Zhang,[20] Z. Y. Zhang,[80] Z. Y. Zhang,[45] Z. Z. Zhang,[47] Zh. Zh. Zhang,[20] G. Zhao,[1] J. Y. Zhao,[1,67] J. Z. Zhao,[1,61] L. Zhao,[1] L. Zhao,[75,61] M. G. Zhao,[45] S. J. Zhao,[84] Y. B. Zhao,[1,61] Y. L. Zhao,[58] Y. X. Zhao,[33,67] Z. G. Zhao,[75,61] A. Zhemchugov,[38,g] B. Zheng,[76] B. M. Zheng,[36] J. P. Zheng,[1,61] W. J. Zheng,[1,67] X. R. Zheng,[20] Y. H. Zheng,[67,j] B. Zhong,[43] C. Zhong,[20] H. Zhou,[37,52,q] J. Q. Zhou,[36] S. Zhou,[6] X. Zhou,[80] X. K. Zhou,[6] X. R. Zhou,[75,61] X. Y. Zhou,[41] Y. X. Zhou,[81] Y. Z. Zhou,[12,f] A. N. Zhu,[67] J. Zhu,[45] K. Zhu,[1] K. J. Zhu,[1,61,67] K. S. Zhu,[12,f] L. Zhu,[36] L. X. Zhu,[67] S. H. Zhu,[74] T. J. Zhu,[12,f] W. D. Zhu,[12,f] W. J. Zhu,[1] W. Z. Zhu,[20] Y. C. Zhu,[75,61] Z. A. Zhu,[1,67] X. Y. Zhuang,[45] J. H. Zou,[1] and J. Zu[75,61]

(BESIII Collaboration)

[1]*Institute of High Energy Physics, Beijing 100049, People's Republic of China*
[2]*Beihang University, Beijing 100191, People's Republic of China*
[3]*Bochum Ruhr-University, D-44780 Bochum, Germany*
[4]*Budker Institute of Nuclear Physics SB RAS (BINP), Novosibirsk 630090, Russia*
[5]*Carnegie Mellon University, Pittsburgh, Pennsylvania 15213, USA*
[6]*Central China Normal University, Wuhan 430079, People's Republic of China*
[7]*Central South University, Changsha 410083, People's Republic of China*
[8]*China Center of Advanced Science and Technology, Beijing 100190, People's Republic of China*
[9]*China University of Geosciences, Wuhan 430074, People's Republic of China*
[10]*Chung-Ang University, Seoul, 06974, Republic of Korea*

[11]*COMSATS University Islamabad, Lahore Campus, Defence Road, Off Raiwind Road, 54000 Lahore, Pakistan*
[12]*Fudan University, Shanghai 200433, People's Republic of China*
[13]*GSI Helmholtzcentre for Heavy Ion Research GmbH, D-64291 Darmstadt, Germany*
[14]*Guangxi Normal University, Guilin 541004, People's Republic of China*
[15]*Guangxi University, Nanning 530004, People's Republic of China*
[16]*Guangxi University of Science and Technology, Liuzhou 545006, People's Republic of China*
[17]*Hangzhou Normal University, Hangzhou 310036, People's Republic of China*
[18]*Hebei University, Baoding 071002, People's Republic of China*
[19]*Helmholtz Institute Mainz, Staudinger Weg 18, D-55099 Mainz, Germany*
[20]*Henan Normal University, Xinxiang 453007, People's Republic of China*
[21]*Henan University, Kaifeng 475004, People's Republic of China*
[22]*Henan University of Science and Technology, Luoyang 471003, People's Republic of China*
[23]*Henan University of Technology, Zhengzhou 450001, People's Republic of China*
[24]*Hengyang Normal University, Hengyang 421001, People's Republic of China*
[25]*Huangshan College, Huangshan 245000, People's Republic of China*
[26]*Hunan Normal University, Changsha 410081, People's Republic of China*
[27]*Hunan University, Changsha 410082, People's Republic of China*
[28]*Indian Institute of Technology Madras, Chennai 600036, India*
[29]*Indiana University, Bloomington, Indiana 47405, USA*
[30a]*INFN Laboratori Nazionali di Frascati, INFN Laboratori Nazionali di Frascati, I-00044, Frascati, Italy*
[30b]*INFN Sezione di Perugia, I-06100, Perugia, Italy*
[30c]*University of Perugia, I-06100, Perugia, Italy*
[31a]*INFN Sezione di Ferrara, INFN Sezione di Ferrara, I-44122, Ferrara, Italy*
[31b]*University of Ferrara, I-44122, Ferrara, Italy*
[32]*Inner Mongolia University, Hohhot 010021, People's Republic of China*
[33]*Institute of Modern Physics, Lanzhou 730000, People's Republic of China*
[34]*Institute of Physics and Technology, Mongolian Academy of Sciences, Peace Avenue 54B, Ulaanbaatar 13330, Mongolia*
[35]*Instituto de Alta Investigación, Universidad de Tarapacá, Casilla 7D, Arica 1000000, Chile*
[36]*Jilin University, Changchun 130012, People's Republic of China*
[37]*Johannes Gutenberg University of Mainz, Johann-Joachim-Becher-Weg 45, D-55099 Mainz, Germany*
[38]*Joint Institute for Nuclear Research, 141980 Dubna, Moscow region, Russia*
[39]*Justus-Liebig-Universitaet Giessen, II. Physikalisches Institut, Heinrich-Buff-Ring 16, D-35392 Giessen, Germany*
[40]*Lanzhou University, Lanzhou 730000, People's Republic of China*
[41]*Liaoning Normal University, Dalian 116029, People's Republic of China*
[42]*Liaoning University, Shenyang 110036, People's Republic of China*
[43]*Nanjing Normal University, Nanjing 210023, People's Republic of China*
[44]*Nanjing University, Nanjing 210093, People's Republic of China*
[45]*Nankai University, Tianjin 300071, People's Republic of China*
[46]*National Centre for Nuclear Research, Warsaw 02-093, Poland*
[47]*North China Electric Power University, Beijing 102206, People's Republic of China*
[48]*Peking University, Beijing 100871, People's Republic of China*
[49]*Qufu Normal University, Qufu 273165, People's Republic of China*
[50]*Renmin University of China, Beijing 100872, People's Republic of China*
[51]*Shandong Normal University, Jinan 250014, People's Republic of China*
[52]*Shandong University, Jinan 250100, People's Republic of China*
[53]*Shandong University of Technology, Zibo 255000, People's Republic of China*
[54]*Shanghai Jiao Tong University, Shanghai 200240, People's Republic of China*
[55]*Shanxi Normal University, Linfen 041004, People's Republic of China*
[56]*Shanxi University, Taiyuan 030006, People's Republic of China*
[57]*Sichuan University, Chengdu 610064, People's Republic of China*
[58]*Soochow University, Suzhou 215006, People's Republic of China*
[59]*South China Normal University, Guangzhou 510006, People's Republic of China*
[60]*Southeast University, Nanjing 211100, People's Republic of China*
[61]*State Key Laboratory of Particle Detection and Electronics, Beijing 100049, Hefei 230026, People's Republic of China*
[62]*Sun Yat-Sen University, Guangzhou 510275, People's Republic of China*
[63]*Suranaree University of Technology, University Avenue 111, Nakhon Ratchasima 30000, Thailand*

[64]*Tsinghua University, Beijing 100084, People's Republic of China*
[65a]*Turkish Accelerator Center Particle Factory Group, Istinye University, 34010, Istanbul, Turkey*
[65b]*Near East University, Nicosia, North Cyprus, 99138, Mersin 10, Turkey*
[66]*University of Bristol, H H Wills Physics Laboratory, Tyndall Avenue, Bristol, BS8 1TL, United Kingdom*
[67]*University of Chinese Academy of Sciences, Beijing 100049, People's Republic of China*
[68]*University of Groningen, NL-9747 AA Groningen, The Netherlands*
[69]*University of Hawaii, Honolulu, Hawaii 96822, USA*
[70]*University of Jinan, Jinan 250022, People's Republic of China*
[71]*University of Manchester, Oxford Road, Manchester, M13 9PL, United Kingdom*
[72]*University of Muenster, Wilhelm-Klemm-Strasse 9, 48149 Muenster, Germany*
[73]*University of Oxford, Keble Road, Oxford OX13RH, United Kingdom*
[74]*University of Science and Technology Liaoning, Anshan 114051, People's Republic of China*
[75]*University of Science and Technology of China, Hefei 230026, People's Republic of China*
[76]*University of South China, Hengyang 421001, People's Republic of China*
[77]*University of the Punjab, Lahore-54590, Pakistan*
[78a]*University of Turin and INFN, University of Turin, I-10125, Turin, Italy*
[78b]*University of Eastern Piedmont, I-15121, Alessandria, Italy*
[78c]*INFN, I-10125, Turin, Italy*
[79]*Uppsala University, Box 516, SE-75120 Uppsala, Sweden*
[80]*Wuhan University, Wuhan 430072, People's Republic of China*
[81]*Yantai University, Yantai 264005, People's Republic of China*
[82]*Yunnan University, Kunming 650500, People's Republic of China*
[83]*Zhejiang University, Hangzhou 310027, People's Republic of China*
[84]*Zhengzhou University, Zhengzhou 450001, People's Republic of China*

(Received 19 December 2025; accepted 27 March 2026; published 29 April 2026; corrected 15 July 2026)

Using e^+e^- collision data collected with the BESIII detector corresponding to an integrated luminosity of 44.2 fb^{-1}, we measure the Born cross sections for the process $e^+e^- \to \Xi(1530)^0\bar{\Xi}^0 + \text{c.c.}$ at 48 center-of-mass energies between 3.51 and 4.95 GeV. The potential signal from non-$D\bar{D}$ decays for $\psi(3770)$, i.e., $\psi(3770) \to \Xi(1530)^0\bar{\Xi}^0 + c.c.$, is investigated by fitting the dressed cross section, no obvious signal is found. The upper limit of $\mathcal{B}(\psi(3770) \to \Xi(1530)^0\bar{\Xi}^0)$ at 90% confidence level is given.

DOI: 10.1103/j99f-d2l1

[a]Deceased.
[b]Also at the Novosibirsk State University, Novosibirsk, 630090, Russia.
[c]Also at State Key Laboratory of Nuclear Physics and Technology, Peking University, Beijing 100871, People's Republic of China.
[d]Also at MOE Frontiers Science Center for Rare Isotopes, Lanzhou University, Lanzhou 730000, People's Republic of China.
[e]Also at Lanzhou Center for Theoretical Physics, Lanzhou University, Lanzhou 730000, People's Republic of China.
[f]Also at Key Laboratory of Nuclear Physics and Ion-beam Application (MOE) and Institute of Modern Physics, Fudan University, Shanghai 200443, People's Republic of China.
[g]Also at the Moscow Institute of Physics and Technology, Moscow 141700, Russia.
[h]Also at Guangdong Provincial Key Laboratory of Nuclear Science, Institute of Quantum Matter, South China Normal University, Guangzhou 510006, China.
[i]Also at School of Physics and Electronics, Hunan University, Changsha 410082, China.
[j]Also at Hangzhou Institute for Advanced Study, University. of Chinese Academy of Sciences, Hangzhou 310024, China.
[k]Also at Goethe University Frankfurt, 60323 Frankfurt am Main, Germany.
[l]Also at the Department of Mathematical Sciences, IBA, Karachi 75270, Pakistan.
[m]Present address Silesian University in Katowice, Chorzow, 41-500, Poland.
[n]Also at the NRC "Kurchatov Institute," PNPI, 188300, Gatchina, Russia.
[o]Also at Ecole Polytechnique Federale de Lausanne (EPFL), CH-1015 Lausanne, Switzerland.
[p]Also at Key Laboratory for Particle Physics, Astrophysics and Cosmology, Ministry of Education; Shanghai Key Laboratory for Particle Physics and Cosmology; Institute of Nuclear and Particle Physics, Shanghai 200240, People's Republic of China.
[q]Also at Helmholtz Institute Mainz, Staudinger Weg 18, D-55099 Mainz, Germany.

Published by the American Physical Society under the terms of the Creative Commons Attribution 4.0 International license. Further distribution of this work must maintain attribution to the author(s) and the published article's title, journal citation, and DOI. Funded by SCOAP^3.

I. INTRODUCTION

The first charmonium resonance above $D\bar{D}$ production threshold, $\psi(3770)$, was observed in the 1970s [1]. It decays mostly to $D\bar{D}$ final states as the Okubo-Zweig-Iizuka (OZI) [2–4] rule dictates, while the fractions of hadronic and radiative transitions to lower lying charmonium states and decays into light hadrons are small [5–7]. However, the BES experiment measured the branching fraction for $\psi(3770) \to$ non-$D\bar{D}$ to be $14.7 \pm 3.2\%$ [8–11]. The first observation of a non-$D\bar{D}$ decay channel, $\psi(3770) \to \pi^+\pi^- J/\psi$ [12], was reported by the BES experiment in 2005. Subsequently, the CLEO collaboration observed additional exclusive non-$D\bar{D}$ decays of $\psi(3770)$, including hadronic ($\pi^0\pi^0 J/\psi$ and $\eta J/\psi$ [13]) and radiative transitions ($\gamma\chi_{c0}$ and $\gamma\chi_{c1}$ [14,15]). Recently, the BESIII collaboration reported a first measurement of the branching fraction for the inclusive decay $\psi(3770) \to J/\psi X$ ($X = \pi^+\pi^-$, $\pi^0\pi^0$, η, π^0, $\gamma\gamma$) of $(0.5 \pm 0.2)\%$ [16]. This result is compatible with the sum of the related branching fractions [17] for $\psi(3770) \to \pi^+\pi^- J/\psi$, $\pi^0\pi^0 J/\psi$, $\eta J/\psi$, $\gamma\chi_{cJ}$ with $J = 0, 1, 2$.

Besides the study of the hadronic and radiative transitions to lower lying charmonium states discussed above, the decays $\psi(3770) \to B\bar{B}$ ($B =$ baryon) are of particular interest. Together with other measurements of $\psi(3770)$ non-$D\bar{D}$ decays mentioned above, they offer valuable insights into the nature of the $\psi(3770)$. Up to now, the experimental information on the decays of $\psi(3770)$ into baryon pairs is scarce above the open-charm threshold. Experimental studies [18–30] of the processes $e^+e^- \to B\bar{B}$ were performed from $\sqrt{s} = 3.51$ to 4.95 GeV by the BESIII and Belle experiments. Except for the evidence for $\psi(3770) \to \Lambda\bar{\Lambda}$ [22] and $\psi(3770) \to \Xi^-\bar{\Xi}^+$ [23], there is no evidence for $\psi(3770)$ decaying to octet-decuplet baryon pairs ($B_{10}\bar{B}_8$) [17].

Based on the SU(3)-flavor symmetry, the decays $\psi \to B\bar{B}$ into baryon pairs of the same multiplet are allowed, while the decays $\psi \to B_{10}\bar{B}_8$ are forbidden [31–33]. Nevertheless, violations of these predictions have long been known. For instance, $J/\psi \to \Xi^-\bar{\Xi}(1530)^+$, $J/\psi \to \bar{\Sigma}^+\Sigma(1835)^-$, $J/\psi \to \bar{\Sigma}^-\Sigma(1835)^+$, $\psi(3686) \to \Xi(1530)^+\bar{\Xi}^-$, $\psi(3686) \to \Xi(1530)^0\bar{\Xi}^0$, etc., were reported by the DM2 and BESIII Collaborations [34–38]. Measurement of cross sections of the $e^+e^- \to B_{10}\bar{B}_8$ final states above the open charm threshold and investigations of the $\psi(3770) \to B_{10}\bar{B}_8$ decay will therefore provide additional information to understand the nature of $\psi(3770)$.

This paper reports the measurement of Born cross section for the $e^+e^- \to \Xi(1530)^0\bar{\Xi}^0$ with $\Xi(1530) \to \Xi^-\pi^+$ and $\bar{\Xi}^0 \to \bar{\Lambda}\pi^0$ (charge conjugation is implied throughout this letter) reaction, at cm energies ($\sqrt{s}$) between 3.51 and 4.95 GeV. The measurement uses e^+e^- collision data corresponding to a total integrated luminosity of 44.2 fb^{-1} [39,40], collected by the BESIII detector [41] at the BEPCII collider [42]. In addition, we also search for $\psi(3770)$ in the line shape of the dressed cross section.

II. BESIII DETECTOR AND MONTE CARLO SIMULATION

The BESIII detector records symmetric e^+e^- collisions provided by the BEPCII storage ring in the cm energy from 1.84 GeV to 4.95 GeV, with a peak luminosity of 1.1×10^{33} cm^{-2} s^{-1} achieved at $\sqrt{s} = 3.773$ GeV. BESIII has collected large data samples in this energy region. The cylindrical core of the BESIII detector covers 93% of the full solid angle and consists of a helium-based multilayer drift chamber (MDC), a time-of-flight system (TOF), and a CsI (Tl) electromagnetic calorimeter (EMC), which are all enclosed in a superconducting solenoidal magnet providing a 1.0 T magnetic field. The solenoid is supported by an octagonal flux-return yoke with resistive plate counter muon identification modules interleaved with steel. The charged-particle momentum resolution at 1 GeV/c is 0.5%, and dE/dx resolution is 6% for electrons from Bhabha scattering. The EMC measures photon energies with a resolution of 2.5% (5%) at 1 GeV in the barrel (end cap) region. The time resolution in the plastic scintillator TOF barrel region was 68 ps, while that in the end cap region was 110 ps. The end cap TOF system was upgraded in 2015 using multigap resistive plate chamber technology providing a time resolution of 60 ps, which benefits 64% of the data used in this analysis [43–45].

Monte Carlo (MC) simulated data samples produced with a GEANT4-based [46] package, which includes the geometric description of the BESIII detector and the detector response, are used to determine detection efficiencies and to estimate backgrounds. The simulation models the beam energy spread and initial state radiation (ISR) in the e^+e^- annihilations with the generator KKMC [47,48]. The inclusive MC sample includes the production of open charm processes, the ISR production of vector charmonium (-like) states, and the continuum processes incorporated in KKMC. All particle decays are modeled with EVTGEN [49,50] using branching fractions either taken from the Particle Data Group (PDG) [17], when available, or otherwise estimated with LUNDCHARM [51,52]. Final state radiation (FSR) from charged particles is incorporated using the PHOTOS [53] package. This analysis employs a single-baryon tagging technique in which we tag the $\Xi(1530)^0$ candidate through the decay chain $\Xi(1530)^0 \to \Xi^-\pi^+$, with $\Xi^- \to \Lambda\pi^-$ and $\Lambda \to p\pi^-$, while the $\overline{\Xi^0}$ partner is extracted by the recoil mass spectrum of the tagged $\Xi(1530)^0$ signal.

III. EVENT SELECTION

Charged tracks detected in the MDC are required to be within a polar angle θ range of $|\cos\theta| < 0.93$, where θ is defined with respect to the z axis, which is the symmetry

axis of the MDC. Particle identification (PID) for charged tracks combines measurements of the energy deposited in the MDC dE/dx and the flight time in the TOF to form likelihoods $\mathcal{L}_h$ ($h = p$, K, π) for each hadron (h) hypothesis. Tracks are identified as protons (pions) when the proton (pion) hypothesis has the greatest likelihood, i.e., $\mathcal{L}_{p(\pi)} > \mathcal{L}_K$ and $\mathcal{L}_{p(\pi)} > \mathcal{L}_{\pi(p)}$. The Λ candidates are reconstructed from $p\pi^-$ pairs with an invariant mass within ± 7 MeV/c^2 of the Λ nominal mass [17]. A secondary-vertex fit [54] is performed with all the $p\pi^-$ combinations; those with $\chi^2 < 500$ are kept for further analysis. To further suppress background events, the decay length of the Λ is required to be positive. In the case of multiple candidates, the one with an unconstrained mass closest to the nominal mass is retained. The Ξ^- candidates are reconstructed from $\Lambda\pi^-$ pairs with an invariant mass within ± 6.5 MeV/c^2 of the Ξ^- nominal mass [17]. A secondary-vertex fit is performed with all the $\Lambda\pi^-$ combinations. The candidate with an invariant mass closest to the Ξ^- nominal mass is retained if there is more than one candidate in an event. The decay length of Ξ^- is required to be positive to further suppress background. The $\Xi(1530)^0$ candidates are reconstructed by minimizing $|M_{\Xi^-\pi^+} - M_{\Xi(1530)^0}|$, where the $M_{\Xi^-\pi^+}$ is the invariant mass of $\Xi^-\pi^+$ and $M_{\Xi(1530)^0}$ is the nominal $\Xi(1530)^0$ mass [17] (the method has been validated and will not cause bias for the $\Xi(1530)^0$ signal peak). The mass window of $\Xi(1530)^0$ is optimized to be $|M_{\Xi^-\pi^+} - M_{\Xi(1530)^0}| < 13$ MeV/c^2. Furthermore, the $\bar{\Xi}^0$ mass window is chosen as $|M^{\rm recoil}_{\Xi^-\pi^+} - M_{\bar{\Xi}^0}| < 25$ MeV/c^2, where $M^{\rm recoil}_{\Xi^-\pi^+}$ is the recoil mass of $\Xi^-\pi^+$ and $M_{\bar{\Xi}^0}$ is the nominal $\bar{\Xi}^0$ mass [17]. These mass windows are chosen by optimizing the figure-of-merit (FOM = $S/\sqrt{S+B}$), where S is the number of signal MC events and B is the number of estimated background events from the inclusive MC sample. Figure 1 shows the distribution of $M^{\rm recoil}_{\Xi^-\pi^+}$ versus $M_{\Xi^-\pi^+}$ of the accepted candidates in the data at $\sqrt{s} = 3.773$ GeV. The red horizontal lines denote the $\bar{\Xi}^0$ signal region, the dashed green and pink lines denote the $\bar{\Xi}^0$ and $\Xi(1530)^0$ sideband regions, respectively.

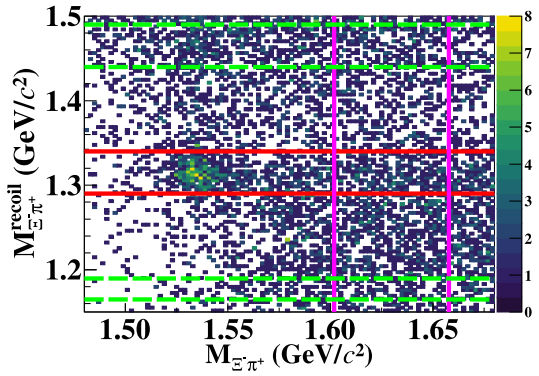


FIG. 1. Distribution of $M^{\rm recoil}_{\Xi^-\pi^+}$ versus $M_{\Xi^-\pi^+}$ of the accepted candidates in data at $\sqrt{s} = 3.773$ GeV. The red lines represent the $\bar{\Xi}^0$ signal region, the dashed-green lines indicate the $\bar{\Xi}^0$ sideband regions, and the pink lines represent the $\Xi(1530)^0$ sideband region.

IV. SIGNAL YIELDS

Two methods are used in this analysis (fitting and counting) to determine the signal yield, depending on the statistics at different energy points. The signal yield at $\sqrt{s} = 3.773$ GeV is obtained by performing a simultaneous fit on the $M_{\Xi^-\pi^+}$ distributions with events in the $\bar{\Xi}^0$ signal and sideband regions. Events in the $\bar{\Xi}^0$ sideband regions are normalized with a scale factor, $R_1 = 0.44$, which is obtained by comparing the number of smooth background events in $\bar{\Xi}^0$ signal and sideband regions, and then fixed in the simultaneous fit. The $\bar{\Xi}^0$ signal region is determined to be $[1.277, 1.352]$ GeV/c^2, and the $\bar{\Xi}^0$ sideband regions are $[1.440, 1.490]$ and $[1.165, 1.190]$ GeV/c^2. Figures 2(a) and 2(b) show the results of the simultaneous fit at $\sqrt{s} = 3.773$ GeV, where the MC-simulated signal shapes are shared for the $\bar{\Xi}^0$ signal and sideband regions in the simultaneous fit.

Due to the low statistics, the signal yield at the other energy points is extracted counting the events as

$$N^{\rm obs} = N^S - R_2 \cdot N^{\rm bkg}, \tag{1}$$

where R_2 is the scale factor related to the $\Xi(1530)^0$ signal and sideband regions in the $M_{\Xi^-\pi^+}$ distribution, determined to 0.52 by using a similar method as for R_1 with the data at $\sqrt{s} = 3.773$ GeV. The $\Xi(1530)^0$ signal and sideband regions are chosen as $[1.511, 1.560]$ GeV/c^2 and $[1.602, 1.658]$ GeV/c^2, respectively; N^S and $N^{\rm bkg}$ are the numbers of events in the above two corresponding regions, obtained by counting as shown in Fig. 2(c), taking $\sqrt{s} = 4.246$ GeV as a sample. Limited by the low statistics, the R_2 values at other cm energy points are assumed to be the same as the one at $\sqrt{s} = 3.773$ GeV. The statistical significance is estimated by $\int_{-s}^{s} 1/\sqrt{2\pi} e^{-x^2/2} dx = 1 - P(N_s)$, where $P(N_s) = 1 - \Sigma_{n=0}^{N_s-1}(b^n/n!)e^{-b}$ is the experimental P value for each energy point, s and b are the number of signal and background events in the signal region. The uncertainty of $N^{\rm obs}$ and its upper limit are computed by the TRolke method [55], and numerical results for all data samples are listed in Table I.

V. CROSS SECTION MEASUREMENT

The Born cross section [58] (σ^B) is the leading-order cross section of a process where the contributions from higher-order electromagnetic processes, such as ISR and vaccum polarization (VP), are excluded via the corresponding correction factors.

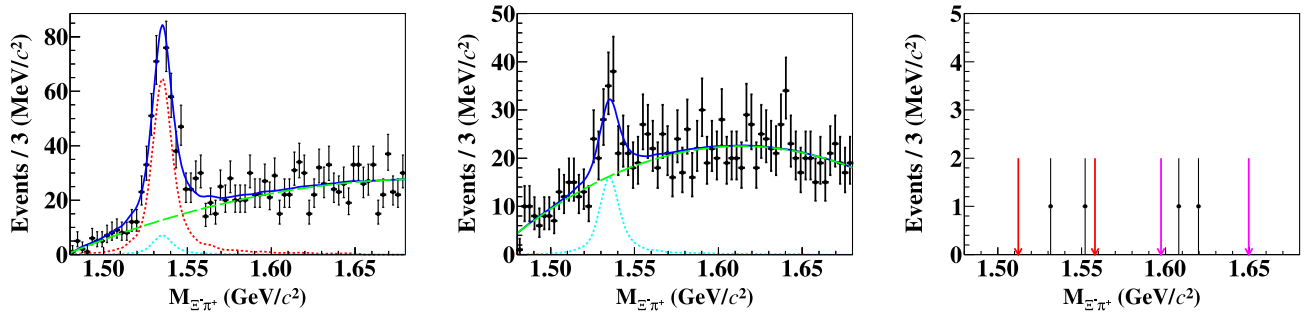


FIG. 2. Simultaneous fit to the $M_{\Xi^-\pi^+}$ distributions in the $\bar{\Xi}^0$ signal (a) and sideband (b) regions for data at $\sqrt{s} = 3.773$ GeV. The dashed green lines indicate the Chebyshev function describing the background shape of the $\bar{\Xi}^0$ signal and sideband regions. The dashed cyan lines indicate the peaking background of $\Xi(1530)^0$ in both $\bar{\Xi}^0$ signal and sideband regions. The dashed red lines indicate the signal shape of $\Xi(1530)^0$. (c) The $M_{\Xi^-\pi^+}$ distribution at $\sqrt{s} = 4.246$ GeV, where the red and pink arrows indicate the $\Xi(1530)^0$ signal and sideband regions, respectively.

The σ^B of the $e^+e^- \to \Xi(1530)^0\bar{\Xi}^0$ process is given by

$$\sigma^B = \frac{N^{\rm obs}}{\mathcal{L}\cdot(1+\delta)\cdot\frac{1}{|1-\Pi|^2}\cdot\epsilon\cdot\mathcal{B}}, \quad (2)$$

where $\mathcal{L}$ is the integrated luminosity, $(1+\delta)$ is the ISR correction factor, $\frac{1}{|1-\Pi|^2}$ is the VP correction factor, ϵ is the selection efficiency, and $\mathcal{B}$ is the product of the branching fractions of $\Xi(1530)^0 \to \Xi^-\pi^+$, $\Xi^- \to \Lambda\pi^-$ and $\Lambda \to p\pi^-$. The VP correction factor is calculated according to Ref. [59]. The ISR correction factor is determined with an iterative weighting method [60].

To study the possible decay $\psi(3770) \to \Xi(1530)^0\bar{\Xi}^0$, a maximum-likelihood fit is performed to the obtained dressed cross section ($\sigma^{\rm dressed} = \sigma^B \cdot \frac{1}{|1-\Pi|^2}$), where the dressed cross section is obtained by including the contribution from the VP effects in the Born cross section. The baseline model $\sigma^{\rm dressed}(\sqrt{s})$ is written as

$$\left| A\cdot\sqrt{p(\sqrt{s})}\cdot\frac{1}{\sqrt{s^N}} + e^{i\phi}BW(\sqrt{s};m,\Gamma,\Gamma_{e^+e^-}\mathcal{B})\cdot\sqrt{\frac{p(\sqrt{s})}{p(M)}}\right|^2. \quad (3)$$

Here, the first term is a power-law (PL) function, in the second term BW is used to describe the resonance. Defined as

$$BW(\sqrt{s}) = \frac{\sqrt{12\pi\Gamma_{e^+e^-}\mathcal{B}(R\to\Xi(1530)^0\bar{\Xi}^0)\Gamma}}{s - M^2 + iM\Gamma}, \quad (4)$$

$p(\sqrt{s})$ is the two-body phase space (PHSP) factor, A and N are parameters of the PL function. In the fit, A, N, the relative phase ϕ, and the product of the electronic partial width and the branching fraction of the resonance decaying into the $\Xi(1530)^0\bar{\Xi}^0$ final state [$\Gamma_{ee}\mathcal{B}(R \to \Xi(1530)^0\bar{\Xi}^0)$] are free parameters. The mass M and the total width Γ are fixed to the $\psi(3770)$ resonance parameters from the PDG [17]. The left plot in Fig. 3 shows the result of the fit to the dressed cross sections with only the PL function, whereas the right plot shows the result for adding an extra assumed $\psi(3770)$ amplitude. The fit parameters with only the PL function are $A = 24.4 \pm 22.6, N = 8.0 \pm 0.7$. Table II shows the parameters with an additional assumed $\psi(3770)$ amplitude for the two solutions. Here, the possible solutions are evaluated based on a two-dimensional scan method, which scans all the pairs of $\Gamma_{e^+e^-}\mathcal{B}$ and ϕ in the parameter space. The significance of the assumed $\psi(3770)$ resonance is calculated by comparing the likelihood values with and without involving the $\psi(3770)$ resonance in the fit and taking the change of the number of degrees of freedom into account. No obvious signal is found. Using the Bayesian method [61], the upper limit of the $\Gamma_{ee}\mathcal{B}[\psi(3770) \to \Xi(1530)^0\bar{\Xi}^0]$ is determined with systematic uncertainty taken into account. Specifically, a scan of the $\Gamma_{ee}\mathcal{B}[\psi(3770) \to \Xi(1530)^0\bar{\Xi}^0]$ with a step of 1×10^{-11} is performed to get the normalized likelihood distribution ($\mathcal{L}$). Then the upper limit on $\Gamma_{ee}\mathcal{B}[\psi(3770) \to \Xi(1530)^0\bar{\Xi}^0]$ is determined by the condition $\Delta\mathcal{L} = 2.706$, which corresponds to the 90% confidence level (CL). Here, $\Delta\mathcal{L}$ is defined as the difference between the likelihood at the upper limit of 90% CL. and its minimum value, and the value of $\Delta\mathcal{L}$ is the 90^{th} percentile of the likelihood distribution with one degree of freedom. Considering the effect on the upper limit from the uncertainty of the resonance parameters, we vary the mass and width of $\psi(3770)$ by $\pm 1\sigma$ and choose the largest upper limit of the $\Gamma_{ee}\mathcal{B}[\psi(3770) \to \Xi(1530)^0\bar{\Xi}^0]$. Then the upper limit of the $\mathcal{B}(\psi(3770) \to \Xi(1530)^0\bar{\Xi}^0)$ is determined to be 6.9×10^{-5}, via dividing the upper limit $\Gamma_{ee}\mathcal{B}[\psi(3770) \to \Xi(1530)^0\bar{\Xi}^0]$ by the leptonic width of $\psi(3770)$.

TABLE I. Numerical results for the dressed cross sections of $e^+e^- \to \Xi(1530)^0\bar{\Xi}^0$ at different energy points [56,57]. Upper limits on $N^{\rm obs}$ and $\sigma^{\rm dressed}$ at 90% confidence level (CL) are listed in parentheses if the significances are less than 3σ. The first uncertainties are statistical and the second are systematic. The $S(\sigma)$ is the statistical significance of the signal.

$\sqrt{s}$ (GeV)	$\mathcal{L}$ (pb^{-1})	N^S	$N^{\rm bkg}$	$N^{\rm obs}$	$\frac{1}{\lvert 1-\Pi\rvert^2}$	$(1+\delta)\cdot\epsilon$	$\sigma^{\rm dressed}(fb)$	$S(\sigma)$
3.510	405.7	29	15	$21.2^{+5.6}_{-4.6}$	1.045	0.13	$471.4^{+124.5}_{-102.3} \pm 47.6$	4.4
3.554	129.4	12	1	$11.5^{+3.9}_{-2.9}$	1.041	0.14	$722.9^{+245.2}_{-182.3} \pm 73.0$	3.3
3.582	85.7	3	2	$2.0^{+2.6}_{-1.3}(<5.1)$	1.039	0.13	$207.2^{+269.3}_{-135.0} \pm 21.0(<529.5)$	1.3
3.650	410.0	12	2	$11.0^{+4.4}_{-3.3}$	1.021	0.15	$215.4^{+86.2}_{-64.6} \pm 21.8$	3.2
3.670	84.7	1	0	$1.0^{+2.3}_{-0.8}(<3.7)$	1.011	0.14	$100.1^{+230.2}_{-80.1} \pm 10.1(<370.3)$	1.0
3.682	404.0	26	14	$18.7^{+4.6}_{-4.0}$	1.021	0.14	$385.3^{+94.8}_{-82.4} \pm 38.9$	4.1
3.768	415.8	8	6	$5.0^{+3.4}_{-2.2}(<8.2)$	1.054	0.14	$97.2^{+66.1}_{-40.8} \pm 9.8(<159.5)$	2.1
3.773	20274.8	···	···	417.4 ± 31.0	1.056	0.14	$172.7^{+12.8}_{-12.8} \pm 17.4$	20.0
3.780	410.0	4	6	$1.0^{+2.3}_{-0.8}(<3.6)$	1.059	0.15	$19.3^{+44.4}_{-15.5} \pm 2.0(<69.6)$	1.3
3.867	108.9	3	0	$3.0^{+2.9}_{-1.6}(<6.9)$	1.051	0.15	$216.5^{+209.3}_{-115.5} \pm 21.9(<498.0)$	1.7
3.871	110.3	3	2	$2.0^{+2.6}_{-1.3}(<5.1)$	1.051	0.14	$154.6^{+201.0}_{-100.5} \pm 15.6(<394.3)$	1.3
4.007	482.0	2	0	$2.0^{+2.6}_{-1.3}(<5.4)$	1.044	0.12	$63.5^{+82.5}_{-41.2} \pm 6.4(<171.3)$	1.4
4.128	401.5	4	1	$3.5^{+2.9}_{-1.6}(<7.5)$	1.052	0.12	$85.7^{+71.0}_{-39.2} \pm 8.7(<183.7)$	1.8
4.157	408.7	2	3	$0.5^{+1.3}_{-0.3}(<2.7)$	1.051	0.13	$11.3^{+29.5}_{-6.8} \pm 1.1(<61.3)$	0.9
4.178	3189.0	38	12	$31.8^{+6.7}_{-5.6}$	1.054	0.13	$90.1^{+19.0}_{-15.9} \pm 9.1$	5.4
4.188	526.7	3	0	$3.0^{+2.9}_{-1.6}(<6.9)$	1.056	0.13	$51.5^{+49.8}_{-27.5} \pm 5.2(<118.4)$	1.7
4.198	526.0	0	1	$-0.5^{+1.3}_{-0.3}(<1.2)$	1.056	0.14	$-7.7^{+20.1}_{-4.6} \pm 0.8(<18.5)$	0.0
4.209	517.1	6	1	$5.5^{+3.4}_{-2.1}(<10.3)$	1.057	0.13	$99.4^{+61.4}_{-37.9} \pm 10.0(<186.1)$	2.3
4.218	514.6	3	0	$3.0^{+2.9}_{-1.6}(<6.9)$	1.056	0.13	$53.9^{+52.1}_{-28.7} \pm 5.4(<123.9)$	1.7
4.226	1100.9	3	2	$2.0^{+2.6}_{-1.3}(<5.1)$	1.057	0.14	$14.8^{+19.3}_{-9.6} \pm 1.5(<37.8)$	1.3
4.235	530.3	1	0	$1.0^{+2.3}_{-0.8}(<3.7)$	1.056	0.13	$17.0^{+39.1}_{-13.6} \pm 1.7(<62.9)$	1.0
4.243	538.1	2	2	$1.0^{+2.3}_{-0.8}(<3.6)$	1.056	0.13	$16.7^{+39.1}_{-13.3} \pm 1.7(<60.0)$	1.0
4.258	828.4	1	0	$1.0^{+2.3}_{-0.8}(<3.7)$	1.054	0.14	$15.5^{+35.6}_{-12.4} \pm 1.6(<57.3)$	1.0
4.266	531.1	3	2	$2.0^{+2.6}_{-1.3}(<5.1)$	1.053	0.13	$34.2^{+44.5}_{-22.2} \pm 3.5(<87.3)$	1.3
4.277	175.7	0	0	$0.0^{+1.8}_{-0.0}(<2.0)$	1.054	0.14	$0^{+87.3}_{-0} \pm 0(<97.0)$	0.0
4.287	502.4	3	2	$2.0^{+2.6}_{-1.3}(<5.1)$	1.053	0.11	$41.5^{+53.9}_{-27.0} \pm 4.2(<105.8)$	1.3
4.312	501.2	2	1	$1.5^{+2.3}_{-0.8}(<4.5)$	1.052	0.11	$31.0^{+47.6}_{-16.5} \pm 3.1(<93.1)$	1.2
4.337	505.0	0	1	$-0.5^{+1.3}_{-0.3}(<1.2)$	1.051	0.13	$-9.1^{+23.7}_{-5.5} \pm 0.9(<21.9)$	0.0
4.358	544.0	1	0	$1.0^{+2.3}_{-0.8}(<3.7)$	1.051	0.14	$15.4^{+35.4}_{-12.3} \pm 1.6(<56.9)$	1.0
4.377	522.7	0	0	$0.0^{+1.8}_{-0.0}(<2.0)$	1.051	0.13	$0^{+32.1}_{-0} \pm 0(<35.7)$	0.0
4.396	507.8	2	1	$1.5^{+2.3}_{-0.8}(<4.5)$	1.051	0.11	$31.0^{+47.5}_{-16.5} \pm 3.1(<92.9)$	1.2
4.415	1090.7	1	3	$-0.6^{+1.3}_{-0.3}(<1.1)$	1.052	0.14	$-4.7^{+10.3}_{-2.4} \pm 0.5(<8.7)$	0.5
4.436	569.9	2	0	$2.0^{+2.6}_{-1.3}(<5.4)$	1.054	0.11	$37.0^{+48.1}_{-24.1} \pm 3.7(<100.0)$	1.0
4.467	111.1	0	0	$0.0^{+1.8}_{-0.0}(<2.0)$	1.055	0.13	$0^{+141.5}_{-0} \pm 0(<157.2)$	0.0
4.527	112.1	0	0	$0.0^{+1.8}_{-0.0}(<2.0)$	1.055	0.13	$0^{+142.8}_{-0} \pm 0(<158.7)$	0.0
4.600	586.9	0	1	$-0.5^{+1.3}_{-0.3}(<1.2)$	1.055	0.13	$-7.8^{+20.2}_{-4.7} \pm 0.8(<18.6)$	0.0
4.611	103.7	0	0	$0.0^{+1.8}_{-0.0}(<2.0)$	1.055	0.11	$0^{+186.3}_{-0} \pm 0(<207.0)$	0.0
4.628	521.5	2	0	$2.0^{+2.6}_{-1.3}(<5.3)$	1.054	0.09	$48.7^{+63.3}_{-31.7} \pm 4.9(<129.1)$	1.0
4.640	551.7	2	0	$2.0^{+2.6}_{-1.3}(<5.4)$	1.054	0.09	$45.4^{+59.0}_{-29.5} \pm 4.6(<122.6)$	1.0
4.661	529.4	1	0	$1.0^{+2.3}_{-0.8}(<3.7)$	1.054	0.09	$23.9^{+54.9}_{-19.1} \pm 2.4(<88.3)$	1.0
4.681	1667.4	2	1	$1.5^{+2.6}_{-1.3}(<4.5)$	1.039	0.09	$11.7^{+20.2}_{-10.1} \pm 1.2(<35.0)$	1.2
4.700	535.5	0	0	$0.0^{+1.8}_{-0.0}(<2.0)$	1.055	0.10	$0^{+37.7}_{-0} \pm 0(<41.9)$	0.0
4.740	163.9	0	0	$0.0^{+1.8}_{-0.0}(<2.0)$	1.055	0.12	$0^{+110.2}_{-0} \pm 0(<122.4)$	0.0
4.750	366.6	1	0	$1.0^{+2.3}_{-0.8}(<3.7)$	1.054	0.12	$26.8^{+61.7}_{-21.4} \pm 2.7(<99.2)$	1.0
4.780	511.5	0	0	$0.0^{+1.8}_{-0.0}(<2.0)$	1.055	0.11	$0^{+36.1}_{-0} \pm 0(<40.2)$	0.0
4.843	525.2	1	0	$1.0^{+2.3}_{-0.8}(<3.7)$	1.056	0.10	$23.4^{+53.7}_{-18.7} \pm 2.4(<86.4)$	1.0
4.918	207.8	0	0	$0.0^{+1.8}_{-0.0}(<2.0)$	1.056	0.11	$0^{+92.0}_{-0} \pm 0(<104.5)$	0.0
4.950	159.3	0	0	$0.0^{+1.8}_{-0.0}(<2.0)$	1.056	0.10	$0^{+128.5}_{-0} \pm 0(<142.8)$	0.0

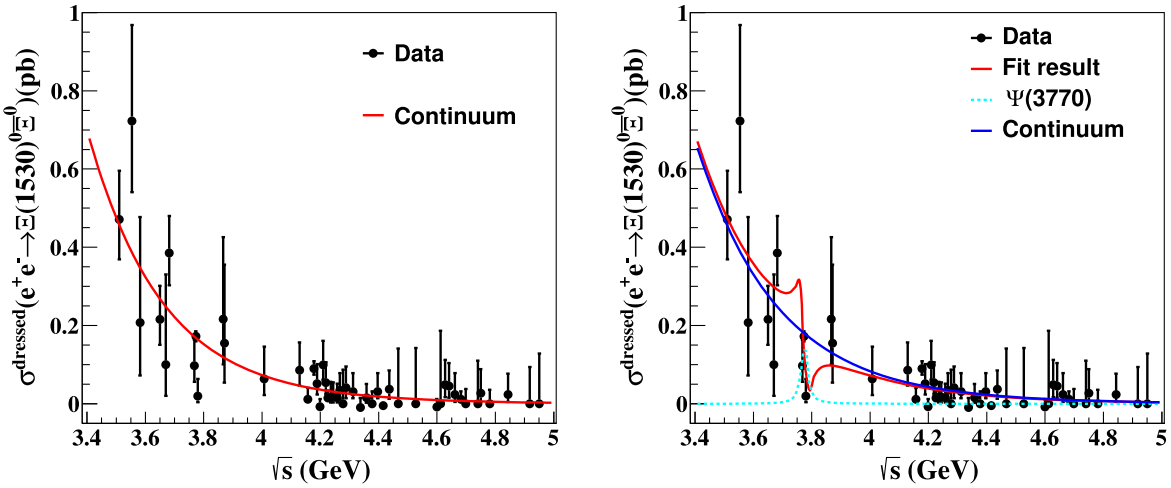


FIG. 3. Fits to the dressed cross section of $e^+e^- \to \Xi(1530)^0\bar{\Xi}^0$ with the assumption of a PL function (left plot) and a PL function plus a $\psi(3770)$ resonance (right plot). The dots with error bars are the dressed cross sections, the red solid lines are the fit results.

VI. SYSTEMATIC UNCERTAINTIES

The sources of the systematic uncertainties in the BCS (Born cross section) measurement are detailed below.

The integrated luminosities of each energy point are measured using the Bhabha events, which have uncertainties of about 1.0% below 4.0 GeV [62], 0.7% from 4.0 to 4.6 GeV [63], and 0.5% above 4.6 GeV [64].

The uncertainties caused by the π^+ tracking [coming from the $\Xi(1530)^0$ mother particle] and PID are investigated with a control sample of $\psi(3686) \to \pi^+\pi^- p\bar{p}$ events. The observed difference in the efficiencies between data and MC simulation, 1.0%, is assigned as the uncertainty for the tracking or PID. The uncertainty of the Ξ^- reconstruction is estimated to be 5.1% with a control sample of $\psi(3686) \to \Xi^-\bar{\Xi}^+$ [65] including the efficiency of the tracking/PID, and Λ reconstruction, the decay length of Λ/Ξ and mass window of Λ/Ξ. The uncertainty due to the $\Xi(1530)^0$ mass window is estimated by fitting the distributions of $M_{\Xi^-\pi^+}$ from data and MC simulation The difference in the accepted efficiencies between data and MC simulation, 3.6%, is taken as the uncertainty. It is worth noting that this uncertainty is only valid for the data samples with low statistics, but not for $\sqrt{s} = 3.773$ GeV, whose signal yield is obtained from the simultaneous fit. The uncertainty due to the $\bar{\Xi}^0$ mass window is estimated by fitting the distributions of $M^{\text{recoil}}_{\Xi^-\pi^+}$ from data and MC simulation. The difference in the accepted efficiencies between data and MC simulation, 2.3%, is taken as the uncertainty. The MC models for the signal channel require the angular-distribution parameters of the baryon pairs as input. The uncertainty due to the angular distribution of the $e^+e^- \to \Xi(1530)^0\bar{\Xi}^0$ process is investigated by changing the model from PHSP to J2BB3 [49,50]. The resulting differences of 3.7% for $\Xi(1530)^0$ and 4.9% for $\bar{\Xi}(1530)^0$ are taken as the uncertainties.

TABLE II. Fitted resonance parameters for $\Gamma_{ee}\mathcal{B}$ and ϕ (rad) with the two solutions. The errors include both statistical and systematic uncertainties.

$\psi(3770)$	$\Gamma_{ee}\mathcal{B}(10^{-3}$ eV)	$\phi(rad)$
Solution I	$13.3 \pm 6.8 (< 18.8)$	-2.0 ± 0.4
Solution II	3.7 ± 6.2	-2.6 ± 0.4

The uncertainty due to the scale factors (R_1, R_2) is caused by the fit parameters when determining the scale factors, and it is estimated by generating multidimensional Gaussian random numbers using the covariance matrix values from the fit as input. The standard deviation of the resultant number of $\Xi(1530)^0$ events, 1.1%, is taken as the systematic uncertainty. The uncertainty introduced by the wrong combination of the π^+ from the $\Xi(1530)^0$ decay is assessed by comparing the signal yields with and without the corresponding component included in the fit. The difference in the cross section, 2.1%, is taken as the uncertainty.

The uncertainty of the input cross section line shape includes two parts: (i) the uncertainty of the input line shape of the cross sections, (ii) the uncertainty of the assumed resonance parameters. For part (i), the input line shape can be varied by changing the parameters, which are used in the fit function, as random numbers satisfying Gaussian distributions. Here, we use the line shape after four iterations as the nominal value, we sample it 200 times according to its error matrix, and perform a Gaussian fit on the sampling results. The width of the Gaussian function is taken as the corresponding systematic uncertainty. For part (ii), the uncertainty is estimated by varying the mass and width of $\psi(3770)$ by $\pm 1\sigma$ with respect to the PDG [17] values. Then, the difference of the $\mathcal{B}(\psi(3770) \to \Xi(1530)^0\bar{\Xi}^0)$ with the nomimal value is taken as the systematic

TABLE III. Total systematic uncertainties (%) and their sources for each energy point on BCS measurement. Here, the combined uncertainty from each item is determined with the assumption that the ratio between the signal yield from tagging $\Xi(1530)^0$ and tagging $\bar{\Xi}(1530)^0$ is 1:1.

$\sqrt{s}$ (GeV)	3.510 → 3.768	3.773	3.780 → 4.530	4.600 → 4.946
Luminosity	1.0	1.0	0.7	0.5
Tracking	1.0	1.0	1.0	1.0
PID	1.0	1.0	1.0	1.0
Ξ^- reconstruction	5.1	5.1	5.1	5.1
Λ mass window	0.3	0.3	0.3	0.3
Λ decay length	0.1	0.1	0.1	0.1
Ξ^- mass window	1.3	1.3	1.3	1.3
Ξ^- decay length	0.5	0.5	0.5	0.5
$\Xi(1530)^0$ mass window	3.6	⋯	3.6	3.6
$\bar{\Xi}^0$ mass window	2.3	2.3	2.3	2.3
Scale factors	1.1	1.1	1.1	1.1
Wrong combinations	2.1	2.1	2.1	2.1
Angular distribution	4.3	4.3	4.3	4.3
Input lineshape	3.9	3.9	3.9	3.9
$\mathrm{Br}(\Xi(1530)^0 \to \Xi^-\pi^+)$	3.7	3.7	3.7	3.7
$\mathrm{Br}(\Xi^- \to \Lambda\pi^-)$	0.0	0.0	0.0	0.0
$\mathrm{Br}(\Lambda \to p\pi^-)$	0.8	0.8	0.8	0.8
Total	10.1	9.5	10.1	10.1

uncertainty. The total systematic uncertainty due to the input line shape is the quadratic sum of these two parts.

The uncertainties due to the quoted branching fractions of the intermediate decays $\Xi(1530)^0 \to \Xi^-\pi^+$, $\Xi^- \to \Lambda\pi^-$ and $\Lambda \to p\pi^-$, are 3.7%, 0.0% and 0.8% [17], respectively, where the 3.7% uncertainty of the branching fraction of $\Xi(1530)^0 \to \Xi^-\pi^+$ is conservatively taken as the upper limit for the branching fraction of $\Xi(1530) \to \gamma\Xi$ [17].

The total systematic uncertainty in the BCS measurements at each energy point is obtained by summing the individual contributions in quadrature, under the assumption that these sources are independent, and is listed in Table III.

VII. SUMMARY

Using a data sample of e^+e^- collisions with a total integrated luminosity of 44.2 fb^{-1} collected with the BESIII detector at the BEPCII collider, the BCS for the process $e^+e^- \to \Xi(1530)^0\bar{\Xi}^0$ is measured by a single-baryon tagging technique, at 48 center-of-mass energies between 3.51 and 4.95 GeV. In order to estimate the possible contribution from the resonance $\psi(3770)$, a fit to the dressed cross sections for $e^+e^- \to \Xi(1530)^0\bar{\Xi}^0$ under the assumption of a resonance $\psi(3770)$ amplitude plus a continuum contribution is performed. No statistically significant evidence is found. The products of branching fractions and electronic partial widths for $\psi(3770)$ decaying into $\Xi(1530)^0\bar{\Xi}^0$, as well as their upper limits at 90% CL are provided for the first time. The result of this work provides new experimental information on the $B\bar{B}$ pair production, as well as the non-$D\bar{D}$ decay for $\psi(3770)$. This study, together with searches for exclusive $\psi(3770) \to B\bar{B}$ decays previously, provides valuable insights into the nature of the $\psi(3770)$.

ACKNOWLEDGMENTS

The BESIII Collaboration thanks the staff of BEPCII [66] and the IHEP computing center for their strong support. This work is supported in part by the National Key R&D Program of China under Contracts No. 2025YFA1613900, No. 2023YFA1606000, and No. 2023YFA1606704; the National Natural Science Foundation of China (NSFC) under Contracts No. 12475197, No. 12275067, No. 11635010, No. 11935015, No. 11935016, No. 11935018, No. 12025502, No. 12035009, No. 12035013, No. 12061131003, No. 12192260, No. 12192261, No. 12192262, No. 12192263, No. 12192264, No. 12192265, No. 12221005, No. 12225509, No. 12235017, and No. 12361141819; the Chinese Academy of Sciences (CAS) Large-Scale Scientific Facility Program; the Strategic Priority Research Program of Chinese Academy of Sciences under Contract No. XDA0480600; CAS under Contract No. YSBR-101; 100 Talents Program of CAS; The Institute of Nuclear and Particle Physics (INPAC) and Shanghai Key Laboratory for Particle Physics and Cosmology; ERC under Contract No. 758462; the German Research Foundation DFG under Contract No. FOR5327; Istituto Nazionale di Fisica Nucleare, Italy; the Knut and Alice Wallenberg Foundation under Contracts No. 2021.0174, No. 2021.0299; the Ministry of Development of Turkey under Contract

No. DPT2006K-120470; the National Research Foundation of Korea under Contract No. NRF-2022R1A2C1092335; Natural Science Foundation of Henan Province under Contract No. 262300421060; Science and Technology R&D Program Joint Fund Project of Henan Province under Contract No. 225200810030; Science and Technology Innovation Leading Talent Support Program of Henan Province under Contract No. 254200510039; Henan Province Foreign Scientists Studio under Contract No. GZS2020032; the National Science and Technology fund of Mongolia; Polish National Science Centre under Contract No. 2024/53/B/ST2/00975; STFC (United Kingdom); the Swedish Research Council under Contract No. 2019.04595; the U.S. Department of Energy under Contract No. DE-FG02-05ER41374.

DATA AVAILABILITY

The data that support the findings of this article are not publicly available because they are owned by a third party and the terms of use prevent public distribution. The data are available from the authors upon reasonable request.

[1] P. A. Rapidis *et al.* (MARKI Collaboration), Phys. Rev. Lett. **39**, 526 (1977).
[2] S. Okubo, Phys. Lett. **5**, 165 (1963).
[3] G. Zweig, An SU3 model for strong interaction symmetry and its breaking, CERN Reports No. CERN-TH-401 and No. CERN-TH-412.
[4] J. Iizuka, Prog. Theor. Phys. Suppl. **37**, 21 (1966).
[5] E. Eichten, K. Gottfried, T. Kinoshita, J. B. Kogut, K. D. Lane, and T. M. Yan, Phys. Rev. Lett. **34**, 369 (1975).
[6] E. Eichten, K. Gottfried, T. Kinoshita, K. D. Lane, and T. M. Yan, Phys. Rev. D **21**, 203 (1980).
[7] X. F. Wang, X. Liu, and Y. N. Gao, Rev. Mod. Phys. **98**, 021001 (2026).
[8] M. Ablikim *et al.* (BES Collaboration), Phys. Lett. B **641**, 145 (2006).
[9] M. Ablikim *et al.* (BES Collaboration), Phys. Rev. Lett. **97**, 121801 (2006).
[10] M. Ablikim *et al.* (BES Collaboration), Phys. Rev. D **76**, 122002 (2007).
[11] M. Ablikim *et al.* (BES Collaboration), Phys. Lett. B **659**, 74 (2008).
[12] J. Z. Bai *et al.* (BES Collaboration), Phys. Lett. B **605**, 63 (2005).
[13] N. E. Adam *et al.* (CLEO Collaboration), Phys. Rev. Lett. **96**, 082004 (2006).
[14] B. A. Briere *et al.* (CLEO Collaboration), Phys. Rev. D **74**, 031106 (2006).
[15] T. E. Coans *et al.* (CLEO Collaboration), Phys. Rev. Lett. **96**, 182002 (2006).
[16] M. Ablikim *et al.* (BESIII Collaboration), Phys. Rev. Lett. **127**, 082002 (2021).
[17] S. Navas *et al.* (Particle Data Group), Phys. Rev. D **110**, 030001 (2024).
[18] M. Ablikim *et al.* (BESIII Collaboration), Phys. Rev. D **87**, 112011 (2013).
[19] M. Ablikim *et al.* (BESIII Collaboration), Phys. Rev. Lett. **120**, 132001 (2018).
[20] M. Ablikim *et al.* (BESIII Collaboration), Phys. Rev. Lett. **124**, 032002 (2020).
[21] H. Liu, J. Zhang, and X. Wang, Symmetry **15**, 214 (2023).
[22] M. Ablikim *et al.* (BESIII Collaboration), Phys. Rev. D **104**, L091104 (2021).
[23] M. Ablikim *et al.* (BESIII Collaboration), J. High Energy Phys. 11 (2023) 228.
[24] M. Ablikim *et al.* (BESIII Collaboration), J. High Energy Phys. 11 (2024) 062.
[25] M. Ablikim *et al.* (BESIII Collaboration), J. High Energy Phys. 07 (2024) 258.
[26] M. Ablikim *et al.* (BESIII Collaboration), Phys. Lett. B **820**, 136557 (2021).
[27] M. Ablikim *et al.* (BESIII Collaboration), Phys. Rev. D **103**, 012005 (2021).
[28] M. Ablikim *et al.* (BESIII Collaboration), J. High Energy Phys. 11 (2025) 111.
[29] M. Ablikim *et al.* (BESIII Collaboration), Phys. Rev. D **111**, L051502 (2025).
[30] M. Ablikim *et al.* (BESIII Collaboration), J. High Energy Phys. 05 (2024) 022.
[31] H. Kowalski and T. F. Walsh, Phys. Rev. D **14**, 852 (1976).
[32] D. M. Asner *et al.*, Int. J. Mod. Phys. A **24**, 499 (2009).
[33] L. Köpke and N. Wermes, Phys. Rep. **174**, 67 (1989).
[34] P. Henrard *et al.* (DM2 Collaboration), Nucl. Phys. **B292**, 670 (1987).
[35] M. Ablikim *et al.* (BESIII Collaboration), Phys. Rev. D **101**, 012004 (2020).
[36] M. Ablikim *et al.* (BESIII Collaboration), Phys. Rev. D **93**, 072003 (2016).
[37] M. Ablikim *et al.* (BESIII Collaboration), Phys. Rev. D **100**, 051101(R) (2019).
[38] M. Ablikim *et al.* (BESIII Collaboration), Phys. Rev. D **104**, 092012 (2021).
[39] M. Ablikim *et al.* (BESIII Collaboration), Chin. Phys. C **39**, 093001 (2015).
[40] M. Ablikim *et al.* (BESIII Collaboration), Chin. Phys. C **46**, 113003 (2022).
[41] M. Ablikim *et al.* (BESIII Collaboration), Nucl. Instrum. Methods Phys. Res., Sect. A **614**, 345 (2010).
[42] M. Ablikim *et al.* (BESIII Collaboration), Chin. Phys. C **44**, 040001 (2020).

[43] X. Li *et al.*, Radiat. Detect. Technol. Methods **1**, 13 (2017).
[44] Y. X. Guo *et al.*, Radiat. Detect. Technol. Methods **1**, 15 (2017).
[45] P. Cao *et al.*, Nucl. Instrum. Methods Phys. Res., Sect. A **953**, 163053 (2020).
[46] S. Agostinelli *et al.*, Nucl. Instrum. Methods Phys. Res., Sect. A **506**, 250 (2003).
[47] S. Jadach, B. F. L. Ward, and Z. Was, Comput. Phys. Commun. **130**, 260 (2000).
[48] S. Jadach, B. F. L. Ward, and Z. Was, Phys. Rev. D **63**, 113009 (2001).
[49] R. G. Ping, Chin. Phys. C **32**, 599 (2008).
[50] D. J. Lange, Nucl. Instrum. Methods Phys. Res., Sect. A **462**, 152 (2001).
[51] J. C. Chen, G. S. Huang, X. R. Qi, D. H. Zhang, and Y. S. Zhu, Phys. Rev. D **62**, 034003 (2000).
[52] R. L. Yang, R. G. Ping, and H. Chen, Chin. Phys. Lett. **31**, 061301 (2014).
[53] E. Richter-Was, Phys. Lett. B **303**, 163 (1993).
[54] M. Xu *et al.* (BESIII Collaboration), Chin. Phys. C **33**, 428 (2009).
[55] J. Lundberg, J. Conrad, W. Rolke, and A. Lopez, Comput. Phys. Commun. **181**, 683 (2010).
[56] M. Ablikim *et al.* (BESIII Collaboration), Chin. Phys. C **40**, 063001 (2016).
[57] M. Ablikim *et al.* (BESIII Collaboration), Chin. Phys. C **45**, 103001 (2021).
[58] M. Inokuti, Rev. Mod. Phys. **43**, 297 (1971).
[59] F. Jegerlehner and R. Szafron, Eur. Phys. J. C **71**, 1632 (2011).
[60] W. Sun, T. Liu, M. Jing, L. Wang, B. Zhong, and W. Song, Front. Phys. (Beijing) **16**, 64501 (2021).
[61] Y. S. Zhu, Chin. Phys. C **32**, 363 (2008).
[62] M. Ablikim *et al.* (BESIII Collaboration), Chin. Phys. C **39**, 093001 (2015).
[63] M. Ablikim *et al.* (BESIII Collaboration), Chin. Phys. C **46**, 113002 (2022).
[64] M. Ablikim *et al.* (BESIII Collaboration), Chin. Phys. C **46**, 113003 (2022).
[65] M. Ablikim *et al.* (BESIII Collaboration), Phys. Rev. Lett. **124**, 032022 (2020).
[66] https://cstr.cn/31109.02.BEPC.

Correction: Minor errors in the caption of Table I and in one of the column headings have been fixed.